Dielectrophoretic Manipulation of Embryonic Nematodes in a Microfluidic System

Khashayar Khoshmanesh [a*], Nimrod Kiss [b], Saeid Nahavandi [a], Clive W. Evans [b], Jonathan M. Cooper [c], David E. Williams [d], Donald Wlodkowic [e*]

[a] Centre for Intelligent Systems Research, Deakin University, Waurn Ponds, Australia;
[b] School of Biological Sciences, University of Auckland, Auckland, New Zealand;
[c] School of Engineering, University of Glasgow, Glasgow, UK;
[d] School of Chemical Sciences, University of Auckland, New Zealand;
[e] The BioMEMS Research Group, School of Chemical Sciences, University of Auckland, New Zealand

ABSTRACT

Small multi-cellular organisms such as nematodes are emerging models for a variety of biomedical applications. Small size, optical transparency of organs, ease of culture, and the capability to develop and respond to environmental parameters make them attractive models for a variety of cellular, genetic and pharmacological studies. This work demonstrates the unique features of dielectrophoresis, the induced motion of polarisable particles in non-uniform electric fields, to manipulate embryonic nematodes in a microfluidic platform. The system took advantage of curved chromium/gold microelectrodes patterned on a glass slide to produce dielectrophoresis, and a polymeric microchamber integrated onto the glass slide to harbour nematodes. The microchamber was filled with a 200 µm of nematode sample while the microelectrodes were energised with an AC signal of 8-10 V_{p-p} and 20 MHz. The nematodes eggs exhibited positive dielectrophoretic response, and were immobilised at the delta-shaped region between the curved microelectrodes within 10-15 minutes. After immobilisation process, the magnitude of AC signal was reduced to 3-4 V_{p-p} to minimise the negative impact of electric field, facilitate the normal embryo development, and eventually hatching of nematode eggs within 2-6 hours. The trapping force was not strong enough to immobilise the nematode worms at the microelectrodes. However, reducing the frequency to 0.1-1 MHz led to immediate immobilisation and stretching of worms between the microelectrodes. The demonstrated system enables the real-time, non-invasive imaging of developing multi-cellular organisms, and studying the response of eggs/worms to different chemical stimuli.

1. INTRODUCTION

Small multicellular organisms such as nematodes ans zebrafish are emerging models for biomedical and environmental studies [1]. Small size, optical transparency of organs and embryos, ease of culture, short geenration time, and avilability make them ideal models for large scale genetic and pharmacological studies, modeling of human diseases and studying behavior at the neuronal level [2, 3]. Furthermore, there are a large number of environmental and toxicological experiments that can only be performed using small model organisms [4].

Despite of these hugh demands, the manipulation and immobilisation of micron-sized multicellular organisms is still a challenging task due to the intristic limitations of conventional benth-top systems. Recent advances in microfabrication technology have enabled the development of highly controllable micro-environments for the immobilisation, cultivation, phenotyping, stimulation and imaging of small multicellular organisms [5]. These technologies are particularly advantageous as they offer a wide range of automated functionalities [1, 6, 7]. Among these technologies are the microfluidic chambers, clamps, pneumatic valves, microsuction manifolds, thermal and chemical immobilization and segmented flow, which have been mainly applied for studying the behaviour of *Caenorhabditis elegans (C. Elegance)* worms [8-12].

* **Corresponding authors:** khashayar.khoshmanesh@deakin.edu.au & d.wlodkowic@auckland.ac.nz

Dieelectrophoresis, the induced motion of neutral particles in a non-uniform electric field can be applied for the trapping and immaging of micron-sized muti-cellular organisms [13]. The response of the particles within a DEP filed depends on their polarisation relative to the surrounding medium, which can be readily controlled by adjusting the electrical conductivity of the medium and the frequency of the AC signal applied to the microelectrodes. If the particle is more polarised than the surrounding medium, the particle is pushed towards the microelectrdoes and such a motion is called positive DEP. Alternatively, if the the particle is less polarised than the surrounding medium, the particle is pushed away from the microelectrdoes and such a motion is called negative DEP [14, 15]. Dielectrophoresis has already widespread applicaions for manipulation, sorting, trapping and characterisation of mamalian cells [16-18], yeasts [19], bacteria [20, 21], viruses [22] and even cell organelles [23].

In this work, we demonstrate the unique capabilities of a DEP-based microfluidic system for the manipulation of an Antarctic nematode known as *Panagrolaimus davidi (P. Davidi)* [24]. The behaviour of the DEP system is analysed using finite volume-based numerical simulations, while the response of eggs and worms to the DEP field is modelled using the single-shell ellipsoidal model. We show the immobilising of eggs and worms between the curved microelectrodes before and after pre-filtering of worms from the sample. The response of worms is analysed at different frequencies of the applied AC signal. The capability of the DEP system for the dynamic analysis of developmental stages of embryonic eggs is shown by trapping and time lapse imaging of eggs. Further, we investigate the response of trapped worms to methanol.

2. MATERIALS AND METHODS

The DEP platform consists of a glass substrate that supports two independent sets of curved microelectrode arrays on its surface. To fabricate the microelectrodes, a thin film of chromium was deposited on the substrate with a thickness of 500 Å to serve as adhesive layer followed by a gold film with a thickness of 1500 Å using the electron beam evaporation process. The pattern of the microelectrodes was realised using photolithography techniques [16]. The AC signal was applied through the interconnecting pads (6×2.25 mm) patterned on the glass slide. Copper wires were bonded to the pads using conductive silver-filled adhesive (Epoxy Technology, Inc., USA) (Figure 1A). Next, we applied a non-contact, CO_2 laser cutting system to create two elliptic chambers within a poly-methyl methacrylate (PMMA) block. A thin layer of polydImethylsyloxane (PDMS) was later used as the adhesive layer to bond the PMMA block to the DEP platform (Figure 1A).

The nematode *P.davidi* was originally collected from the McMurdo Sound region in Antarctica and was maintained in vitro as a parthenogenetic strain [24, 25]. Nematodes were grown at 15-20ºC on standard nematode growth medium (NGM) agar plates seeded with *E. coli* as a food source. Embryonated eggs, larval stages and adults were rinsed from culture plates with distilled water (DI) and filtered through a 40 µm cell strainer to separate the embryonated eggs from hatched stages.

The microelectrodes were energised using a function generator (BK Precision 4087, B&K Precision Corporation, USA). Images were acquired using a motorized Nikon Eclipse TiE (Nikon Corporation, Japan) epifluorescence microscope equipped with a cooled DS-Qi1Mc CDD camera (Nikon). Automated time-lapse image acquisition was used for up to eight hours using NIS-Elements AR software (Nikon) (Figure 1B).

A

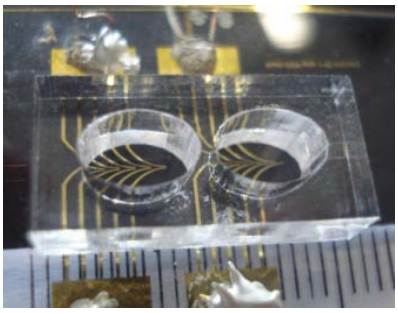

B

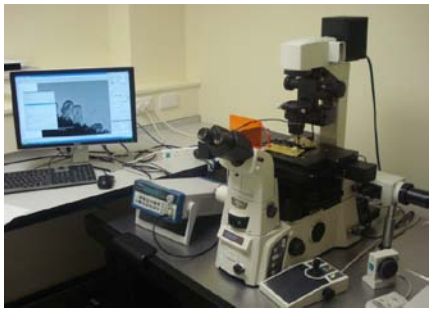

Figure 1. Experimental setup of the microfluidic system: (A) Close-up view of DEP platform equipped with curved microelectrodes patterned on a glass slide and a PMMA block which accommodates two elliptical chambers, (B) External interfaces including the microscope, function generator and computer.

3. GOVERNING EQUATIONS

Considering the eggs and worms as ellipsoidal structures, the time-averages DEP force imposed on them is calculated as below [13, 26]:

$$F_{DEP} = \pi r^2 L \cdot \varepsilon_{med} \cdot \mathrm{Re}[f_{CM}] \cdot \nabla E_{rms}^2 \tag{1}$$

where L and $2r$ are the principal and semi-principal axes of the ellipsoid, ε_{med} is the permittivity of the medium, E_{rms} is the root-mean-square value of the applied electric field, and Re[f_{CM}] is the real part of the Clausius-Mossotti factor.

The f_{CM}, which reflects the polarisation of the bio-particles with respect to the surrounding medium, depends on the dielectric properties of the bio-particles and the surrounding medium, and also on the frequency of the applied AC signal, as defined below [26]:

$$f_{CM} = \frac{1}{3} \frac{\varepsilon^*_{bio-particle} - \varepsilon^*_{med}}{\left[\varepsilon^*_{med} + (\varepsilon^*_{bio-particle} - \varepsilon^*_{med})\, DPF\right]} \tag{2}$$

$$\varepsilon^* = \varepsilon - \frac{i\sigma}{\omega},\ i = \sqrt{-1} \tag{3}$$

$$DPF_L = \frac{1-e^2}{2\,e}\left[\log\left(\frac{1+e}{1-e}\right) - 2e\right] \tag{4}$$

$$DPF_r = \frac{1 - DPF_L}{2} \tag{5}$$

$$e = \sqrt{1 - \left(\frac{2r}{L}\right)^2} \tag{6}$$

where ε^* is the complex permittivity of the bioparticles or the medium, DPF is the deplorization factor, σ is the electrical conductivity of the bioparticles or the medium, ω is the angular frequency of the applied AC signal, and e is the eccentricity of the ellipsoid.

However, the eggs and worms like other biological organisms have a much more complicated structure, comprised of several layers of different materials that are asymmetrically integrated into each other. For simplification, we assume that the eggs and worms consist of a core surrounded by a thin shell, and applied the ellipsoidal single-shell model to approximate the DEP response of the eggs and worms (Figure 2) [26].

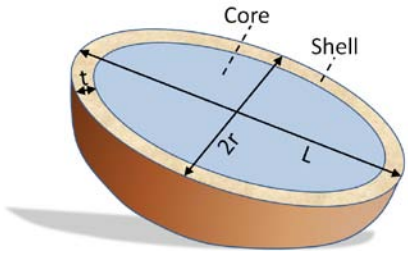

Figure 2. The eggs and worms were assumed to consist of a core wrapped inside a thin shell

In doing so, we first calculated the equivalent f_{CM} of the core-shell structure, and then calculated the f_{CM} of the eggs and worms by considering the core-shell structure surrounded by the suspending medium, as comprehensively described in [13]. The physical properties of the eggs, worms and the medium are summarised in Table 1. The dimensions of eggs and worms are experimentally measured while the dielectric properties of egg's and worm's core and shell were taken as those of cell's interior and plasma membrane [27] and the permittivity of worm's core (body) was taken as that of muscle [28].

Table 1. The physical properties of eggs/worms applied in our ellipsoidal single-shell model

Medium (DI water)		σ_{med} = 5×10^{-4} S/m ε_{med} =*78* ε_o F/m	*N/A*
Eggs	Core	σ_{emb} = 0.5 S/m ε_{emb} =*50* ε_o F/m	*L/D* =1.25, 1.5, 2 D = 57.5±7.5 µm L = 72.5±12.5 µm *t* = 2 µm
	Shell	σ_{shell} = 5×10^{-8} S/m ε_{shell} =*20* ε_o F/m	
Worms	Core	σ_{body} = 0.5 S/m ε_{body} =*112* ε_o F/m	*L/D* =10, 15, 20 D = 17±3 µm L = 212.5±62.5 µm *t* = 0.1 D
	Shell	σ_{skin} = 5×10^{-8} S/m ε_{skin} =*20* ε_o F/m	

Using the above properties, we calculated the Re[f_{CM}] of the eggs and worms, as given in Figure 2. As seen, the DEP response of the eggs and worms was much stronger along their major axis, and more importantly strongly depended on the aspect ratio of the structures. For example, at L/D=1.5, the eggs demonstrated a crossover frequency of 31.5 kHz above which they exhibited positive DEP response. The Re[f_{CM}] reached a peak value of 0.68±0.035 within the frequency range of 0.2-10 MHz, and decreased thereafter until reaching 0.27 at 40 MHz (Figure 3A). In contrast, the worms exhibited positive DEP response across the entire frequency range. For example at L/D=15, the Re[f_{CM}] reached a peak value of 20.1±1.1 within the frequency range of 65-450 kHz, and decreased thereafter until reaching 1.04 at 40 MHz (Figure 3B). Next, we applied equation (1) and the values given in Table (1) to calculate the DEP force applied on *P. davidi* eggs and worms at 20 MHz (Figure 3C). Due to computational limitations, only three pairs of microelectrodes are considered in the model while more details about the simulation can be found in [16, 19, 29]. The maximum trapping force is produced at the tip region of curved microelectrodes, and therefore we expect to immobilise a high density of eggs and worms at this region.

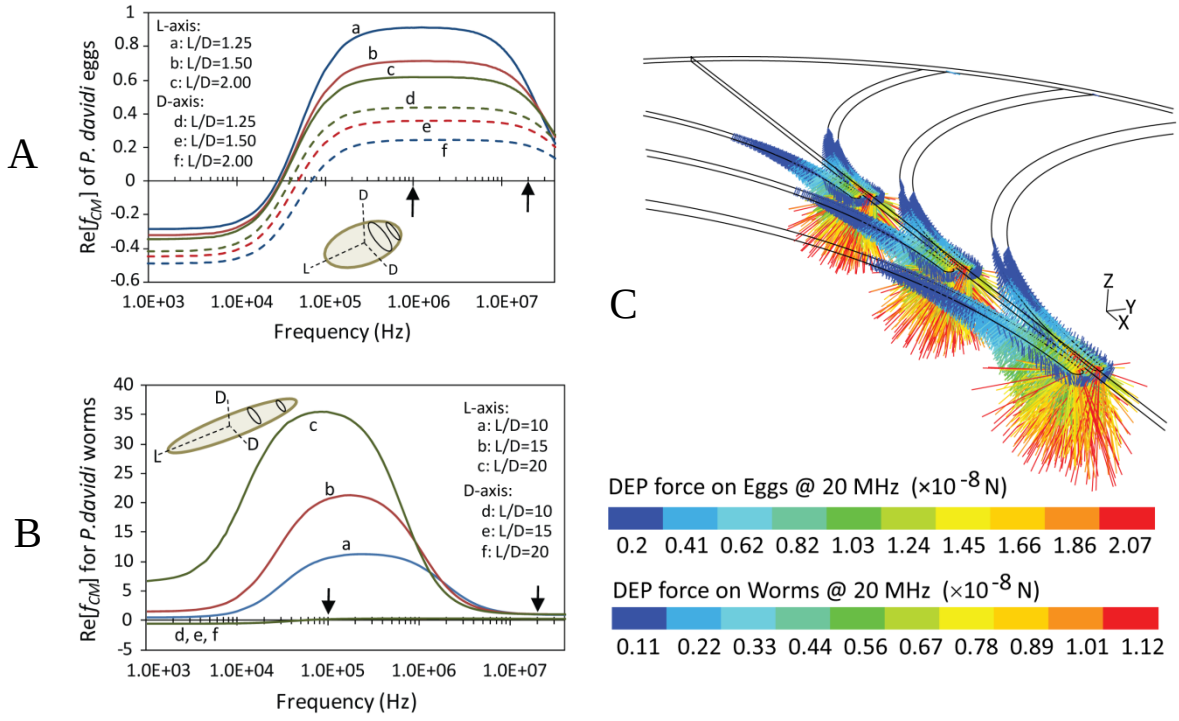

Figure 3. Numerical characterisation of our DEP system: (A) DEP response of fresh *P. davidi* eggs at different aspect ratios, (B) DEP response of juvenile *P. davidi* worms at different aspect ratios, and (C) Distribution of DEP force applied on *P. davidi* eggs and worms.

4. RESULTS AND DISCUSSIONS

4.1. Trapping of eggs and worms

The *P. davidi* eggs and worms were resuspended in DI water of 5×10^{-4} S/m and then 200 µlit of the sample was injected to the PMMA chamber. Microelectrodes were activated with an AC signal of 10 V_{p-p} and 20 MHz. Joule heating and electrolysis were minimized due to the low conductivity of DI water and high frequency of the signal [30]. The eggs were randomly dispersed at the bottom surface of the chamber while the worms freely moved close to the bottom surface (Figure 4A). The sample was pipette 3-5 times to induce vortices within the PMMA chamber and move the eggs and worms. Approaching the microelectrode tips, the eggs and worms were trapped under the positive DEP force. Applying a mixed population of eggs and works led to trapping of both specimens between the microelectrodes (Figure 4B). However, passing the sample through the 40 µm cell strainer prior to application to the PMMA chamber significantly decreased the density of worms and led to a pure population of eggs trapped along the microelectrodes (Figure 4C). The eggs were patterned along the microelectrodes with their major axis oriented along the electric field and characteristic pearl-chains formed between the neighbouring eggs. A few worms remained in the sample even after filtering could move very close to the microelectrodes, however the DEP force was strong enough to overcome the locomotion of worms and keep the eggs at their locations (Figure 4D-F).

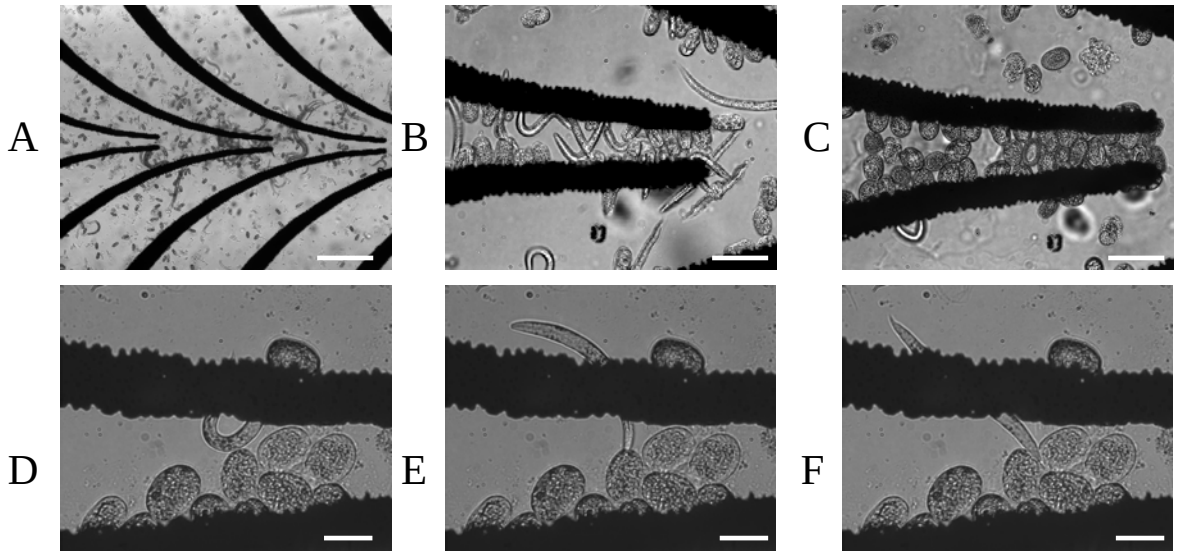

Figure 4. Immobilisation of *P. davidi* eggs and worms in our DEP system: (A) Distribution of specimens immediately after injection to PMMA chamber, bar=500 µm, (B) Trapping a mixed population of eggs and worms, bar=100 µm (C) Trapping eggs from a sample that has been filtered several time to minimise the density of worms, bar=100 µm (D-F) The trapping force was strong enough to overcome the locomotion of worms and anchor them in their positions, bar=75 µm.

4.2. Characterising the response of worms at different frequencies

The trapped eggs were not sensitive to frequency variations, which is in line with our numerical model (Figure 3A). However, the worms were quite sensitive to frequency variations. At frequencies higher than 2 MHz, while the trapping DEP force was not strong enough to immobilise the worms it was sufficient to restrict their locomotion to the microelectrode's surface area where they were retained (Figure 5A-C). The worms remained viable in this condition for up to 15 hours. By contrast, at frequencies lower than 100 kHz the worms were immediately immobilisation and stretched between the microelectrodes (Figure 5D-E). The DEP force at such low frequencies was strong enough to overcome the locomotion of worms, which is consistent with our numerical models (Figure 3B). However, the viability of the worms reduced only 2 hours, either due to a number of events occurring at low frequencies, including temperature rise due to Joule heating effect [25], imposing an intensive transmembrane voltage on the cells and undesired chemical reactions at the surface of microelectrodes or due to the nature of the worms which cannot survive after constraining.

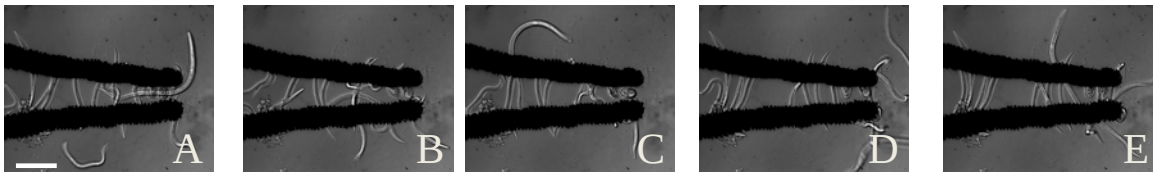

Figure 5. Characterising the DEP response of worms at different frequencies: (A-C) Frequencies higher than 2 MHz did not prevent the locomotion of worms, in contrast (D-E) Frequencies lower than 100 kHz stretched the worms between the microelectrodes, bar=100 μm.

4.3. Imaging the developmental stages of eggs

Next, we assessed the capability of our DEP device for imaging the developmental stages of embryos in a non-synchronised population of *P. davidi* eggs. The sample was filtered via the 40 μm cell strainer to minimise the population of worms before introducing to PMMA chamber. Following the immobilisation process, the magnitude of AC signal was reduced to 3-4 V_{p-p} to minimise the negative impact of electric field. We focused on a population of eggs, which were trapped approximately 1000-1400 μm away from the tips while the microelectrodes were energised at 10 V_{p-p} and 1 MHz (Figure 6). This location was selected as the immobilised eggs experienced a weaker electric field and temperature rise, and could survive over long periods up to 15 hours. The positive DEP force was strong enough to pattern the eggs while it did not affect the embryo development which progressed normally until hatching, as compared with control experiments (Figure 6 A-E). The eggs remained stably immobilised except for some minor displacements caused by the movements of the hatched *P.davidi* worms (Figure 4C).

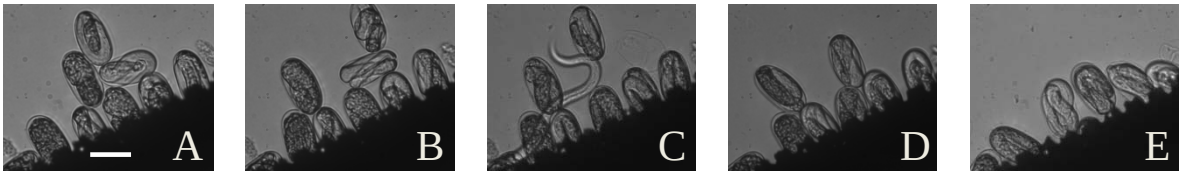

Figure 6. Imaging the developmental stages of *P. davidi* eggs in our DEP device after (A) 15 min, (B) 60 min, (C) 150 min, (D) 180 min and (E) 240 min, bar=100 μm.

4.4. Characterising the response of worms to toxins

Subsequently, we investigated the effect of methanol on trapped *P. davidi* worms. A 200 μlit of the sample containing mostly worms was injected to the PMMA chamber while the microelectrodes were energised with an AC signal of 10 V_{p-p} and 20 MHz. Following the immobilisation of worms, a 30 μlit of methanol was injected to the chamber. While the viable worms demonstrated a snaky configuring, administration of methanol made them to demonstrate a coiled configuration most likely as an intrinsic defensive mechanism, as observed for the free worms which were far from the microelectrodes (Figure 7A-B). Interestingly, the same response was observed for the worms trapped between the microelectrodes and the snaky structure of worms (Figure 5A-C) shifted to coiled structures (Figure 7C). However, lowering the frequency to 50 kHz, stretched the coiled worms (Figure 7D), enabling the analysis of stimulated worms. \

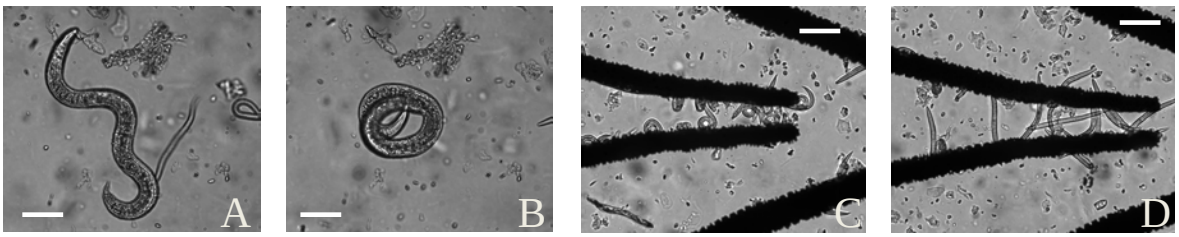

Figure 7. Cauterising the response of *P. davidi* worms to methanol: (A) Viable worms demonstrate a snaky configuration, but (B) demonstrate a coiled configuration after methanol poisoning, (C) Trapped wormed after methanol poisoning at 20 MHz and (D) Decreasing the frequency to 50 MHz stretched the coiled worms, bar=100 μm.

5. CONCLUSIONS

This work demonstrated the capabilities of a DEP-based microfluidic system for the manipulation of *P. davidi* eggs and worms. The polarisation of eggs and worms at different frequencies and aspect ratios was predicted using the single-shell ellipsoidal model while the distribution of DEP within the PMMA chamber was modelled using finite volume-based numerical simulations. We showed the rapid immobilising of eggs and worms between the curved microelectrodes before and after filtration of the sample. Moreover, analysing the response of worms at different frequencies of the applied AC signal proved that the worms can be stretched and remain motionless at frequencies lower than 100 kHz. Furthermore, we showed that DEP system can be applied for the dynamic analysis of developmental stages of embryonic eggs. Finally, we analysed the response of trapped worms to methanol. This work can be applied for a wide range of biomedical and environmental studies on different small multicellular organisms.

ACKNOWLEDGMENT

This work was supported by the Endeavour Research Fellowships, Department of Education, Employment and Workplace Relations, Australia and the Centre for Intelligent Systems Research, Deakin University, Australia (KK); Foundation for Research Science and Technology, New Zealand (DW, DEW); University of Auckland, New Zealand (DW, KK), and BBSRC, EPSRC and Scottish Funding Council, United Kingdom, funded under the RASOR Program (JMC).

REFERENCES

[1] D. Wlodkowic, K. Khoshmanesh, J. Akagi, D. E. Williams, and J. M. Cooper, "Wormometry-on-a-Chip: Innovative Technologies for In Situ Analysis of Small Multicellular Organisms," *Cytometry Part A*, vol. 79A, pp. 799-813, Oct 2011.

[2] S. E. Hulme and G. M. Whitesides, "Chemistry and the Worm: Caenorhabditis elegans as a Platform for Integrating Chemical and Biological Research," *Angewandte Chemie-International Edition*, vol. 50, pp. 4774-4807, 2011 2011.

[3] A. Ben-Yakar, N. Chronis, and H. Lu, "Microfluidics for the analysis of behavior, nerve regeneration, and neural cell biology in C. elegans," *Current Opinion in Neurobiology*, vol. 19, pp. 561-567, Oct 2009.

[4] A. L. Rubinstein, "Zebrafish assays for drug toxicity screening," *Expert Opinion on Drug Metabolism & Toxicology*, vol. 2, pp. 231-240, Apr 2006.

[5] C. B. Rohde, F. Zeng, R. Gonzalez-Rubio, M. Angel, and M. F. Yanik, "Microfluidic system for on-chip high-throughput whole-animal sorting and screening at subcellular resolution," *Proceedings of the National Academy of Sciences of the United States of America*, vol. 104, pp. 13891-13895, Aug 28 2007.

[6] D. Wlodkowic, S. Faley, M. Zagnoni, J. P. Wikswo, and J. M. Cooper, "Microfluidic Single-Cell Array Cytometry for the Analysis of Tumor Apoptosis," *Analytical Chemistry*, vol. 81, pp. 5517-5523, Jul 1 2009.

[7] D. Wlodkowic, K. Khoshmanesh, J. C. Sharpe, Z. Darzynkiewicz, and J. M. Cooper, "Apoptosis goes on a chip: advances in the microfluidic analysis of programmed cell death," *Analytical Chemistry*, vol. 83, pp. 6439-6446, Sep 1 2011.

[8] N. Chronis, M. Zimmer, and C. I. Bargmann, "Microfluidics for in vivo imaging of neuronal and behavioral activity in Caenorhabditis elegans," *Nature Methods*, vol. 4, pp. 727-731, Sep 2007.

[9] P. Rezai, A. Siddiqui, P. R. Selvaganapathy, and B. P. Gupta, "Behavior of Caenorhabditis elegans in alternating electric field and its application to their localization and control," *Applied Physics Letters*, vol. 96, Apr 12 2010.

[10] S. Park, H. Hwang, S.-W. Nam, F. Martinez, R. H. Austin, and W. S. Ryu, "Enhanced Caenorhabditis elegans Locomotion in a Structured Microfluidic Environment," *Plos One*, vol. 3, Jun 25 2008.

[11] S. D. Buckingham and D. B. Sattelle, "Strategies for automated analysis of C-elegans locomotion," *Invertebrate Neuroscience*, vol. 8, pp. 121-131, Sep 2008.

[12] M. M. Crane, K. Chung, J. Stirman, and H. Lu, "Microfluidics-enabled phenotyping, imaging, and screening of multicellular organisms," *Lab on a Chip,* vol. 10, pp. 1509-1517, 2010 2010.

[13] K. Khoshmanesh, N. Kiss, S. Nahavandi, C. W. Evans, J. M. Cooper, D. E. Williams, and D. Wlodkowic, "Trapping and imaging of micron-sized embryos using dielectrophoresis," *Electrophoresis,* pp. n/a-n/a, 2011.

[14] B. Cetin and D. Li, "Dielectrophoresis in microfluidics technology," *Electrophoresis,* vol. 32, pp. 2410-2427, 2011.

[15] K. Khoshmanesh, S. Nahavandi, S. Baratchi, A. Mitchell, and K. Kalantar-zadeh, "Dielectrophoretic platforms for bio-microfluidic systems," *Biosensors & Bioelectronics,* vol. 26, pp. 1800-1814, Jan 15 2011.

[16] K. Khoshmanesh, J. Akagi, S. Nahavandi, J. Skommer, S. Baratchi, J. M. Cooper, K. Kalantar-Zadeh, D. E. Williams, and D. Wlodkowic, "Dynamic Analysis of Drug-Induced Cytotoxicity Using Chip-Based Dielectrophoretic Cell Immobilization Technology," *Analytical Chemistry,* vol. 83, pp. 2133-2144, Mar 15 2011.

[17] I. F. Cheng, C. C. Chung, and H. C. Chang, "High-throughput electrokinetic bioparticle focusing based on a travelling-wave dielectrophoretic field," *Microfluidics and Nanofluidics,* vol. 10, pp. 649-660, Mar 2011.

[18] C. J. Huang, H. C. Chien, T. C. Chou, and G. B. Lee, "Integrated microfluidic system for electrochemical sensing of glycosylated hemoglobin," *Microfluidics and Nanofluidics,* vol. 10, pp. 37-45, Jan 2011.

[19] K. Khoshmanesh, C. Zhang, F. J. Tovar-Lopez, S. Nahavandi, S. Baratchi, K. Kalantar-Zadeh, and A. Mitchell, "Dielectrophoretic-activated cell sorter based on curved microelectrodes," *Microfluidics and Nanofluidics,* vol. Online, pp. DOI 10.1007/s10404-009-0558-7, 2010.

[20] B. H. Lapizco-Encinas, B. A. Simmons, E. B. Cummings, and Y. Fintschenko, "Insulator-based dielectrophoresis for the selective concentration and separation of live bacteria in water," *Electrophoresis,* vol. 25, pp. 1695-1704, Jun 2004.

[21] K. Khoshmanesh, S. Baratchi, F. J. Tovar-Lopez, S. W. Nahavandi, W., A. Mitchell, and K. Kalantar-zadeh, "On-Chip Separation of Lactobacillus Bacteria from Yeasts using Dielectrophoresis," *Microfluidics and Nanofluidics,* vol. Article in press,DOI:10.1007/s10404-011-0900-8, 2012.

[22] F. Grom, J. Kentsch, T. Muller, T. Schnelle, and M. Stelzle, "Accumulation and trapping of hepatitis A virus particles by electrohydrodynamic flow and dielectrophoresis," *Electrophoresis,* vol. 27, pp. 1386-1393, Apr 2006.

[23] M. Moschallski, M. Hausmann, A. Posch, A. Paulus, N. Kunz, T. T. Duong, B. Angres, K. Fuchsberger, H. Steuer, D. Stoll, S. Werner, B. Hagmeyer, and M. Stelzle, "MicroPrep: Chip-based dielectrophoretic purification of mitochondria," *Electrophoresis,* vol. 31, pp. 2655-2663, Aug 2010.

[24] D. A. Wharton, "Osmoregulation in the Antarctic nematode Panagrolaimus davidi," *Journal of Experimental Biology,* vol. 213, pp. 2025-2030, Jun 15 2010.

[25] I. M. Brown, D. A. Wharton, and R. B. Millar, "The influence of temperature on the life history of the Antarctic nematode Panagrolaimus davidi," *Nematology,* vol. 6, pp. 883-890, 2004 2004.

[26] M. Castellarnau, A. Errachid, C. Madrid, A. Juarez, and J. Samitier, "Dielectrophoresis as a tool to characterize and differentiate isogenic mutants of Escherichia coli," *Biophysical Journal,* vol. 91, pp. 3937-3945, Nov 2006.

[27] Y. Huang, S. Joo, M. Duhon, M. Heller, B. Wallace, and X. Xu, "Dielectrophoretic cell separation and gene expression profiling on microelectronic chip arrays," *Analytical Chemistry,* vol. 74, pp. 3362-3371, Jul 2002.

[28] R. Pethig, "Dielectric properties of body tissues," *Clinical physics and physiological measurement : an official journal of the Hospital Physicists' Association, Deutsche Gesellschaft fur Medizinische Physik and the European Federation of Organisations for Medical Physics,* vol. 8 Suppl A, pp. 5-12, 1987 1987.

[29] K. Khoshmanesh, C. Zhang, S. Nahavandi, F. J. Tovar-Lopez, S. Baratchi, A. Mitchell, and K. Kalantar-Zadeh, "Size based separation of microparticles using a dielectrophoretic activated system," *Journal of Applied Physics,* vol. 108, Aug 1 2010.

[30] H. Morgan and N. G. Green, *AC Electrokinetics: colloids and nanoparticles* Baldock: Research Studies Press LTD., 2003.